

## Performance and Stability Limits at Near-Unity Aspect Ratio in the Pegasus Toroidal Experiment

R. Fonck, S. Diem, G. Garstka, M. Kissick, B. Lewicki, C. Ostrander, P. Probert, M. Reinke, A. Sontag, K. Tritz, E. Unterberg

University of Wisconsin, Madison, Wisconsin, USA

E-mail address of main author: [fonck@engr.wisc.edu](mailto:fonck@engr.wisc.edu)

**Abstract:** The Pegasus Toroidal Experiment is a mid-sized extremely-low aspect ratio ( $A$ ) spherical torus (ST). It has the dual roles of exploring limits of ST behavior as  $A$  approaches 1 and studying the physics of ST plasmas in the tokamak-spheromak overlap regime. Major parameters are  $R = 0.25 - 0.45$  m,  $A = 1.1 - 1.4$ ,  $I_p \leq 0.15$  MA, and  $B_T < 0.1$  T. High beta plasmas are produced at very low toroidal field by ohmic heating. Values of toroidal beta  $> 20\%$  have been obtained, and the operational space of beta vs  $I_p/aB_T$  is similar to that observed for NBI-heated START discharges. Achievable plasma current is subject to an apparent limit of  $I_p/I_{tf} \sim 1$ . Access to higher-current plasmas appears to be restricted by the appearance of large internal MHD activity, including  $m/n=2/1$  and  $3/2$  modes. Recent experiments have begun to access ideal stability limits, with disruptions observed as  $q_{95}$  approaches 5, in agreement with numerical predictions for external kink mode onset.

### 1. Introduction

The Pegasus Toroidal Experiment [1] is a mid-sized, extremely low aspect ratio spherical torus. It has the dual roles of exploring the limits of spherical torus plasma behavior as the aspect ratio,  $A$ , approaches unity and of examining alternate confinement concepts in the tokamak-spheromak overlap regime. Unique MHD properties arise with possibilities of strong mode coupling at very high toroidicity. Access to near-unity aspect ratio is achieved through use of a novel high-stress reinforced solenoid magnet assembly [2]. Operation with ohmic heating has started to demonstrate the high- $\beta$  stability capabilities of operation at near-unity aspect ratio. Design parameters are  $R = 0.25 - 0.45$  m,  $A = 1.1 - 1.4$ , elongation = 1 - 3.5,  $I_p \sim 0.15$  MA,  $B_T < 0.1$  T, and  $P_{HHFW} \leq 1$  MW.

### 2. Plasma Equilibrium Characteristics

Global magnetic parameters are obtained through equilibrium reconstruction using a wide array of magnetics diagnostics. The vacuum vessel is continuous and has a skin time on the order of the plasma formation time (several ms). Induced currents in the wall are generally greater than the plasma current, and are estimated with a coupled current-filament model. These estimates are used as inputs to an equilibrium code and are constrained in the reconstruction by measurements from flux loops and B-dot coils. Equilibrium properties are estimated by the code which uses a two-step iterative procedure to reconstruct the equilibria. The Gauss-Seidel multigrid relaxation technique is used to solve the Grad-Shafranov equation for each iteration, between which the Levenberg-Marquardt method is used to minimize  $\chi^2$ . A sample equilibrium is given in Fig 1.

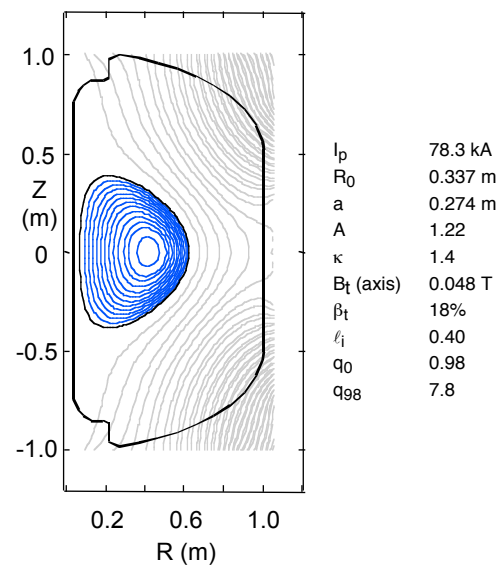


FIG. 1 Pegasus equilibrium reconstruction.

Monte Carlo error analysis indicates that uncertainties in the fitted plasma parameters are determined mainly by diagnostic uncertainties. Over a wide range of plasma parameters, the relative uncertainties are estimated to be  $\sigma(I_p)/I_p = 0.02$ ,  $\sigma(q_0)/q_0 = 0.2$ ,  $\sigma(q_{95})/q_{95} = 0.06$ ,  $\sigma(\beta_t)/\beta_t = 0.15$ ,  $\sigma(l_i)/l_i = 0.09$ , and  $\sigma(S)/S = 0.3$ , where  $S$  is the local magnetic shear in the inner plasma region.

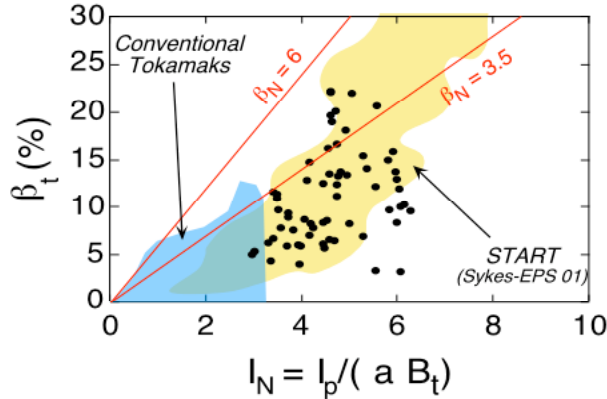


FIG. 2 Toroidal  $\beta_t$  values in ohmic plasmas. Pegasus data is indicated by solid dots.

High  $\beta_t$  plasmas are obtained by operation at very low toroidal field, and cover a regime of  $\beta_t$  vs  $I_N$  space similar to neutral-beam heated high- $\beta_t$  plasmas in START and other ST experiments (Fig. 2)[3]. As indicated,  $\beta_t$  values  $> 20\%$  and  $\beta_N \sim 5$  have been obtained with no evidence of a  $\beta$  limit to date. Densities range up to the Greenwald limit ( $\sim I_p/\pi a^2$ ). Stored energies are consistent with values expected from the ITER98pby1 confinement scaling. Plasma startup is characterized by high current ramp rates (15-45 MA/s), low internal inductance ( $l_i \sim 0.3$ ), and high elongation. The resulting low-

A discharges typically have  $l_i < 0.5$ , which is due to both the low aspect geometry and the fact that the loop voltage continues to increase after initial plasma formation. The plasma paramagnetism rises to 1.25 in the center region.

### 3. Field Utilization Limit and MHD Activity

The toroidal field utilization factor,  $I_p/I_{TF}$ , is a useful parameter for characterizing access to the operational regime between tokamak ( $I_p/I_{TF} \ll 1$ ) and spheromak ( $I_p/I_{TF} \gg 1$ ) regimes. To date,  $I_p/I_{TF}$  has reached values as high as (and slightly exceeding) unity, as shown in Figure 3, but appears to approach an operational boundary at that level. Two factors appear to contribute to this soft limit: 1) plasma startup at low- $B_T$ ; and 2) large-scale internal MHD activity.

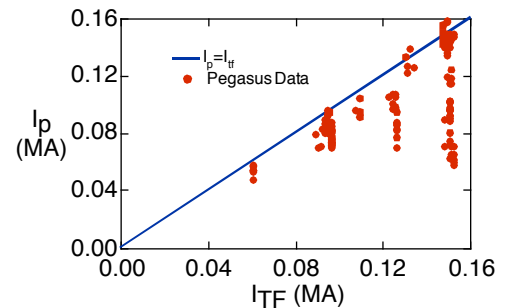


FIG. 3 Plasma current vs. toroidal field rod current

The first factor is the difficulty inherent in plasma startup at increasingly lower toroidal field. This is due both to the effect of field errors at very low  $B_t$  and poorer coupling of the 5.5 GHz preionization source to the breakdown region. Plasma formation occurs later in time as the toroidal field is reduced, reflecting the fact that the loop voltage is increasing in time during the startup phase. The result of this delayed startup is a reduction in flux available for current drive. Flux consumption analyses indicate, however, that this flux reduction accounts for at most 1/3 of the drop in  $I_p$  as  $I_{TF}$  is decreased.

#### 3.1 Internal Tearing Mode Activity

The second factor limiting access to high- $I_p$  plasmas at low  $B_T$  is the presence of significant resistive MHD activity. In almost all high power discharges, an  $m=2/n=1$  mode appears

during the current ramp and can persist for most of the shot duration. This mode rotates in the electron diamagnetic direction with frequencies on the order of a few kHz. The mode is highly non-cylindrical, with 3/4 of the poloidal phase shift observed along the center column. The onset of this 2/1 activity coincides with the development of a large region of low shear near the  $q = 2$  surface (Figs. 4a and 4b) while the plasma is still forming and hence quite resistive. Soft X-ray measurements indicate these modes extend over a large fraction of the plasma core. In plasmas where the 2/1 mode is suppressed by careful discharge tailoring, a 3/2 mode arises following a quiescent period. As the 3/2 mode grows, a weaker 2/1 mode appears to be destabilized, presumably due to profile modification and/or increased toroidal mode coupling. The 2/1 mode is frequently accompanied by harmonic  $n = 2$  and 3 components indicating a high degree of toroidicity. The broad extent of this mode and indications of mode coupling may suggest that these discharges have characteristics combining elements from both the standard tokamak and the more self-organized spheromak regime.

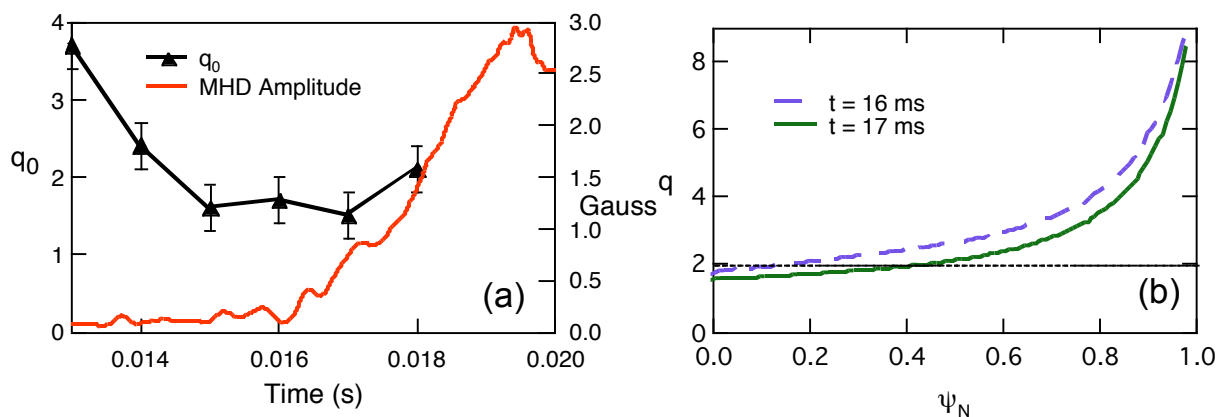


FIG. 4. Characteristics of limiting MHD activity. Signatures of large internal modes: (a)  $q(0)$ , and mode amplitude vs time; (b)  $q(r)$  from equilibrium reconstruction.

This internal activity has a strong impact on plasma performance. At large mode amplitudes, both the internal inductance and stored energy remain low, and the Ejima flux consumption coefficient [4] increases to  $> 0.8$ . In contrast, reduction of this internal MHD activity leads to higher  $l_i$ , an increase of stored energy, and a reduction of the Ejima coefficient to  $\sim 0.4$ , indicating significantly decreased dissipation and better confinement of input energy.

Figure 5 shows a comparison of the normalized fluctuation amplitude for discharges with  $I_p/I_{TF} \sim 1$  (Fig. 3). Here, decreasing MHD amplitude is correlated with increasing toroidal field. In contrast, a relatively constant fluctuation level is found for varying  $I_p$  at constant  $I_{TF}$ . Thus, toroidal field is relatively more important in determining MHD activity.

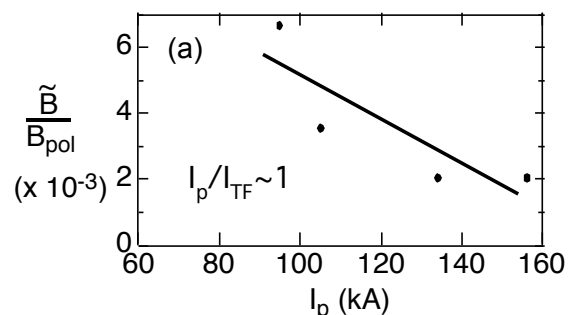


FIG. 5. Internal MHD amplitude vs  $I_p$  for  $I_p \sim I_{TF}$ .

It has been shown that large tearing modes degrade plasma confinement [5]. Since the MHD amplitude is related to the toroidal field, it is reasonable to imply that the increased level of MHD is responsible for the decreased energy confinement and less efficient flux consumption found at lower field. These effects of increased MHD activity appear to be degrading the discharge and contributing to the limit of  $I_p/I_{TF} \sim 1$ .

The operational limit of  $I_p \sim I_{TF}$  thus appears to arise from the development of a wide region of low shear around a low-order rational surface in a resistive plasma. This condition arises quite early in discharges at very low  $A$  and very low  $B_T$ . This supports strong growth of these modes and inhibits further plasma development. The  $I_p \sim I_{TF}$  limit then reflects an operational limit on the  $q(r)$  in the core region.

Near the magnetic axis,  $q_0$  is given by

$$q_0 \approx \frac{2B_t}{\mu_0 R j_0} \frac{1 + \beta^2}{2}$$

A flat current distribution,  $j(r) = j_0$ , gives

$$q_0 \sim \frac{1}{A^2} \frac{I_{TF}}{I_p} \frac{1 + \beta^2}{2} \quad \text{and} \quad \frac{I_p}{I_{TF}} \sim \frac{1}{A^2} \frac{1 + \beta^2}{q_0 \cdot 2}$$

which gives  $I_p \sim I_{TF}$  for typical PEGASUS parameters of  $A \sim 1$ ,  $\beta \sim 1.7$ , and  $q_0 \sim 3/2$  to 2. This is consistent with the existence of a  $q = 2$  rational surface in the interior with low-shear, allowing a large 2/1 mode to grow and degrade plasma confinement and heating efficiency just as  $I_p/I_{TF} \sim 1$ . The appearance of this surface and low shear is observed in the equilibrium reconstructions, supporting this interpretation of the  $I_p/I_{TF} \sim 1$  limit. Both the early development of low-order rational surfaces in the plasma core region, when the plasma is still quite resistive, and the relatively low shear throughout the region contribute to the strong growth of this mode.

#### 4. External Kink Mode Onset

A critical issue for operation at  $A \sim 1$  and low- $B_T$  is the nature of the external kink stability boundary. Pegasus experiments are beginning to access this boundary region, where higher  $I_p$  discharges tend to terminate in abrupt disruptions. Magnetic fluctuations are observed immediately prior ( $\sim 100 \mu\text{s}$ ) to disruption as  $q_{95}$  approaches 5 (Fig. 6). Stability calculations using the VACUUM and DCON codes indicate that the calculated free-boundary energy approaches zero as these oscillations begin; negative energy values here indicate instability to ideal external kink modes. The unstable mode grows on a time scale between the Alfvén time and  $q(dq/dt)^{-1}$ , roughly as expected for a plasma slowly crossing an instability boundary [6]. This onset of an ideal kink mode at relatively high  $q_{95}$  is consistent with expectations that the ideal kink is more virulent at higher edge  $q$  as the aspect ratio approaches unity. [7]

Plasmas with  $\beta \sim 1$  as  $A$  approaches unity in the tokamak-spheromak overlap region appear accessible with the addition of planned new capabilities aimed at lowering the plasma resistivity and manipulating the evolution of the  $q$ -profile to suppress limiting MHD activity. These capabilities include significantly improved control of the plasma position, current, and edge using new switches [8], as well as high harmonic fast wave

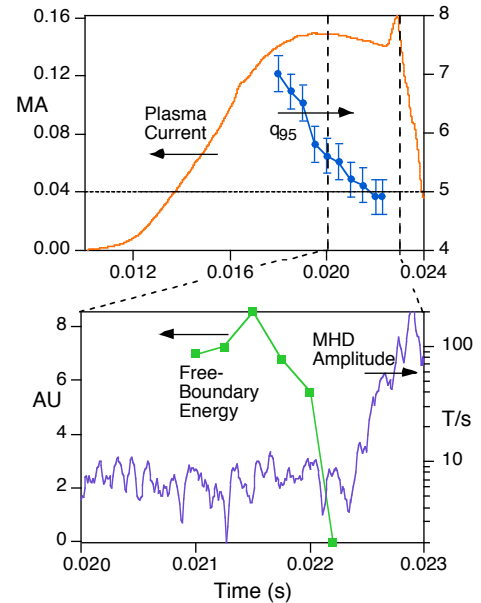


FIG. 6. Signatures of external kink leading to disruption as  $q_{95} \rightarrow 5$ . Top:  $I_p$  and  $q_{95}(t)$ ; Bottom: Mirnov activity and free-boundary energy from DCON.

(HHFW) heating. Control over the ohmic waveform will allow better control over the current profile evolution and provide increased volt-seconds, while radial position control will allow better coupling to the HHFW antenna and control of plasma size. The toroidal field will be increased significantly during startup to avoid low order rational surfaces during the early stages of plasma formation, and reduced later to obtain high  $q$ . TSC modeling of fast  $B_T$  rampdown scenarios indicate accessible paths to regimes of higher current and increased stored energy. Operation with the two-strap high-power Higher Harmonic Fast Wave heating system has begun. Initial loading tests show an impedance of roughly 1 ohm, and power up to 200 KW has been injected into plasma to date.

### Acknowledgement

This work is supported by the U.S. Department of Energy under Grant DE-FG02-96ER54375

### References

- [1] FONCK, R. et al., "Status and Research Plan of the Pegasus Toroidal Experiment", Bull. Am. Phys. Soc. **43** (1998) 1867.
- [2] PERNAMBUKO-WISE, P. et. al., "The Wisconsin Pegasus Solenoid", Physica B **246** (1998) 350.
- [3] SYKES, A., "Overview of Recent Spherical Tokamak Results", Plasma Phys Cont. Fusion **43** (2001) 127.
- [4] EJIMA, S. et al., "Volt-second Analysis and Consumption in Doublet III Plasmas", Nucl. Fusion **22** (1982) 1313.
- [5] CHANG, Z. and CALLEN, J., "Global Energy Confinement Degradation due to Macroscopic Phenomena in Tokamaks", Nuclear Fusion **30** (1990) 219.
- [6] CALLEN, J., et al., "Growth of Ideal Magnetohydrodynamic Modes Driven Slowly through their Instability Threshold: Application to Disruption Precursors", Phys Plasmas **6** (1999) 2963.
- [7] HENDER, T., et al., "Magneto-hydro-dynamic Limits in Spherical Tokamaks", Phys Plasmas **6** (1999) 1958.
- [8] GAUDREAU, M., et al., "Solid-State Pulsed Power Systems", Diversified Technologies Inc. Tech Brief, 23<sup>rd</sup> Int. Power Mod. Symp., Rancho Mirage (1998).